Free Radical Biology and Medicine 126 (2018) 87–100

Contents lists available at ScienceDirect

Free Radical Biology and Medicine

journal homepage: www.elsevier.com/locate/freeradbiomed

Original article

β-Lapachone and its iodine derivatives cause cell cycle arrest at G_2/M phase and reactive oxygen species-mediated apoptosis in human oral squamous cell carcinoma cells

Rosane Borges Dias[a], Taís Bacelar Sacramento de Araújo[a], Raíza Dias de Freitas[a], Ana Carolina Borges da Cruz Rodrigues[a], Letícia Palmeira Sousa[a], Caroline Brandi Schlaepfer Sales[b], Ludmila de Faro Valverde[a], Milena Botelho Pereira Soares[a,c], Mitermayer Galvão dos Reis[a,d], Ricardo Della Coletta[e], Eduardo Antônio Gonçalves Ramos[a,d], Celso Amorim Camara[f], Tania Maria Sarmento Silva[f], José Maria Barbosa Filho[g], Daniel Pereira Bezerra[a,*], Clarissa Araújo Gurgel Rocha[a,h,*]

[a] Gonçalo Moniz Institute, Oswaldo Cruz Foundation (IGM-FIOCRUZ/BA), Salvador, Bahia, Brazil
[b] Department of Biomorphology, Institute of Health Sciences, Federal University of Bahia, Salvador, Bahia, Brazil
[c] Center of Biotechnology and Cell Therapy, Hospital São Rafael, Salvador, Bahia, Brazil
[d] Department of Pathology and Forensic Medicine, School of Medicine of the Federal University of Bahia, Salvador, Bahia, Brazil
[e] Department of Oral Diagnosis, School of Dentistry, University of Campinas, Piracicaba, São Paulo, Brazil
[f] Department of Chemistry, Federal Rural University of Pernambuco, Recife, PE, Brazil
[g] Pharmaceutical Technology Laboratory, Federal University of Paraiba, João Pessoa, Paraíba, Brazil
[h] Laboratory of Oral Surgical Pathology, School of Dentistry of the Federal University of Bahia, Bahia, Brazil

ARTICLE INFO

Keywords:
β-Lapachone
Oral cancer
Chemotherapy
Natural products

ABSTRACT

β-Lapachone is a natural naphthoquinone originally obtained from the bark of the purple Ipe (*Tabebuia avellanedae* Lor, Bignoniaceae) and its therapeutic potential in human cancer cells has been evaluated in several studies. In this study, we examined the effects of β-lapachone and its 3-iodine derivatives (3-I-α-lapachone and 3-I-β-lapachone) on cell proliferation, cell death, and cancer-related gene expression in human oral squamous cell carcinoma cells. β-Lapachone and its 3-iodine derivatives showed potent cytotoxicity against different types of human cancer cell lines. Indeed, treatment with these compounds induced cell cycle arrest at G_2/M phase, followed by internucleosomal DNA fragmentation, and caused significant increases in phosphatidylserine externalization, caspase-8 and -9 activation, mitochondrial membrane depolarization, reactive oxygen species (ROS) production, and apoptotic cell death morphology. The apoptosis induced by the compounds was prevented by pretreatment with a pan-caspase inhibitor (Z-VAD-FMK) and an antioxidant (N-acetyl-L-cysteine). In vivo, β-lapachone and its 3-iodine derivatives significantly reduced tumor burden and did not alter any of the biochemical, hematological, or histological parameters of the animals. Overall, β-lapachone and its 3-iodine derivatives showed promising cytotoxic activity due to their ability to induce cell cycle arrest at G_2/M phase and promote caspase- and ROS-mediated apoptosis. In addition, β-lapachone and its 3-iodine derivatives were able to suppress tumor growth in vivo, indicating that these compounds may be new antitumor drug candidates.

Abbreviations: ctDNA, Calf thymus DNA; CTL, Negative control; DAF-FM diacetate, 4-amino-5-methylamino-2'-,7'-difluofluorescein diacetate; DCF-DA, 2',7'-dichlorodihydrofluorescein diacetate; DMSO, Dimethyl sulfoxide; DOX, Doxorubicin; FBS, Fetal bovine serum; FSC, Forward light scatter; IC_{50}, Half maximal (50%) inhibitory concentration; MAP, Mitogen Activated Protein; NAC, N-acetyl-l-cysteine; OSCC, Oral squamous cell carcinoma; PAS, Periodic Acid Schiff; PBMC, Peripheral blood mononuclear cell; PI, Propidium iodide; ROS, Reactive oxygen species; RQ, relative quantification; SCC, Side scatter; SCID, Severe combined immunodeficiency; SI, selectivity index

* Corresponding authors at: Gonçalo Moniz Institute, Oswaldo Cruz Foundation (IGM-FIOCRUZ/BA), Waldemar Falcão Street, 121, Candeal, 40296-710 Salvador, Bahia, Brazil.

E-mail addresses: daniel.bezerra@fiocruz.br, danielpbezerra@gmail.com (D.P. Bezerra), clarissa.gurgel@fiocruz.br, clarissagurgelrocha@gmail.com (C.A.G. Rocha).

https://doi.org/10.1016/j.freeradbiomed.2018.07.022
Received 14 May 2018; Received in revised form 27 July 2018; Accepted 28 July 2018
Available online 30 July 2018

1. Introduction

Oral cancer is the sixth most frequent cancer worldwide, and oral squamous cell carcinoma (OSCC), as a major type of malignant neoplasm affecting the oral cavity, is the most common histological subtype, accounting for 95% of cases [1,2]. OSCC is a serious global health issue, and it is estimated that more than 500,000 new cases of OSCC are diagnosed and 350,000 OSCC-related deaths occur annually [3].

Recent oncological research has focused on the pathogenesis of cancer, therapeutic targets in cancer, and new pharmacological groups for anticancer treatment. Within this context, natural products represent an important source of new anticancer drugs. Among the pharmacological classes, naphthoquinones such as β-lapachone have attracted the attention of the pharmaceutical industry owing to their diverse biological effects, including cytotoxicity in neoplastic cells [4,5].

β-Lapachone is a natural naphthoquinone originally obtained from the bark of the purple Ipe (*Tabebuia avellanedae* Lor, Bignoniaceae) found in South America. This compound has promising biological activities, including antimicrobial, anti-inflammatory, antimalarial, and anticancer effects [6,7]. β-Lapachone has been evaluated in several studies investigating its therapeutic potential in human cancer cells, and its anticancer activity and mechanisms of action have been extensively studied in several types of cancers, including breast adenocarcinoma [8,9], lung carcinoma [10–12], esophageal carcinoma [4], prostate carcinoma [13,14], hepatocarcinoma [15,16], colorectal carcinoma [17,18], melanoma [19,20], and oral squamous cell carcinoma [21]. Importantly, β-lapachone 3-iodine derivatives such as 3-I-α-lapachone and 3-I-β-lapachone [22,23] have been shown to have anti-inflammatory and antimicrobial properties; however, no studies have demonstrated their anticancer effects.

Therefore, the aim of this study was to evaluate the effects of β-lapachone and its 3-iodine derivatives on cell proliferation, cell death, and cancer-related gene expression in OSCC cells.

2. Materials and methods

2.1. Preparation of β-lapachone and its 3-iodine derivatives

β-Lapachone and its 3-iodine derivatives were obtained as previously described [22,23]. Fig. 1 depicts the chemical structure of β-lapachone and its 3-iodine derivatives.

2.2. Cell culture

Human OSCC cell lines (HSC3, SCC4, SCC9, SCC15 and SCC25), from American Type Culture Collection (ATCC, Manassas, VA, USA), were used in this study. For comparative analysis, we used two immortalized but not transformed cell lines, i.e., HaCaT human normal keratinocytes [24] and MRC5 normal human fibroblasts [25]. In addition to OSCC cell lines, other cell types were also used, as described in Table S1. The cells were cultured in RPMI 1640 medium (Thermo Fisher Scientific, Waltham, MA, USA) with 10% fetal bovine serum (FBS; Thermo Fisher Scientific, Waltham, MA, USA) and 50 μg/mL gentamicin (Novafarma, Anápolis, GO, Brazil) at a temperature of 37 °C in an atmosphere containing 5% CO_2. All cell lines were tested for mycoplasma using a mycoplasma stain kit (Sigma-Aldrich, St. Louis, MO, USA) to validate the use of cells free from contamination.

2.3. PBMC preparation

Human peripheral blood mononuclear cells (PBMCs) were obtained from the peripheral blood of healthy nonsmokers (age 25–35 years), who had not used any drugs or medications for at least 15 days prior to collection. The research ethics committee of the Oswaldo Cruz Foundation (Salvador, Bahia, Brazil) approved the experimental protocol (Approval no. 031019/2013). All participants provided informed consent for participation in the study. Blood collection was performed in heparinized flasks by trained professionals at Fiocruz, Bahia, using sterile and disposable syringes, in a final volume of 5 mL.

PBMCs were isolated by a standard protocol using a Ficoll density gradient (Ficoll-Paque Plus, GE Helthcare Bio-Sciences AB, Sweden). After separation, the cells were washed twice with saline and resuspended (0.3×10^6 cells/mL) in RPMI medium supplemented with 20% FBS, 2 mM glutamine, and 50 μg/mL gentamicin. To induce T lymphocyte cell division, 10 μg/mL concanavalin A (Sigma Chemical Co., St. Louis, MO, USA) was used as a mitogen.

2.4. Cytotoxic activity assay

Cells were cultured in 96-well plates with varying concentrations of β-lapachone and its 3-iodine derivatives for 72 h. Cell viability was measured using Alamar Blue assays, as describe by Ahmed et al. [26], and the absorbance at 570 and 600 nm was measured using a microplate reader (Molecular Devices, Sunnyvale, CA, USA).

2.5. Three-dimensional multicellular spheroid culture

HSC3 cells were cultured in a three-dimensional (3D) model of multicellular cancer spheroids as described by Carvalho et al. [27]. Briefly, cells were seeded in 100-μL aliquots into 96-well plates with a cell-repellent surface (Greiner Bio-One, Kremsmünster, Austria) at a density of 0.5×10^6 cells/mL and cultured in complete medium containing 3% Matrigel (BD Biosciences, San Jose, CA, USA). Spheroids with stable structures had formed after 3 days. The spheroids were then exposed to a range of drug concentrations for 72 h, and cell viability was quantified as described above.

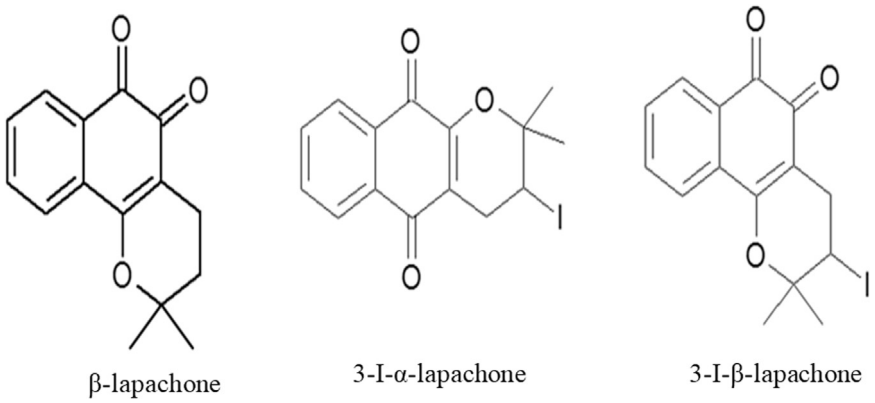

Fig. 1. Chemical structure of β-lapachone and its derivatives, 3-I-α-lapachone and 3-I-β-lapachone.

2.6. Trypan blue exclusion assay

Cellular viability was assessed using trypan blue exclusion assays. Briefly, HSC3 cells were treated with β-lapachone and its 3-iodine derivatives for 12, 24, 48, or 72 h. The numbers of viable and nonviable cells (the latter of which take up trypan blue) were counted. Briefly, 90 μL was removed from the cell suspension, and 10 μL trypan blue (0.4%) was added. Cell counting was performed using a light microscope with a hemocytometer filled with an aliquot of the homogenized cell suspension.

2.7. Internucleosomal DNA fragmentation and cell cycle distribution

Determination of the nuclear DNA content of the cell, which reflects the phases of the cell cycle, was performed by flow cytometry using propidium iodide (PI) as a fluorogenic agent [28]. Cells were harvested in a permeabilization solution containing 0.1% Triton X-100 (Sigma Chemical Co.), 2 μg/mL PI (Sigma Chemical Co.), 0.1% sodium citrate, and 100 μg/mL RNAse (Sigma Chemical Co.) and incubated in the dark for 15 min at room temperature. The fluorescence intensity resulting from attachment of the fluorochrome propidium iodide to DNA is directly proportional to amount of genetic material present in the cell nucleus, representing the distribution of populations cells in different phases of cell cycle. The internucleosomal DNA fragmentation is represented by the amount of cells in sub-G_1, being an indicator of cell death. Finally, cell fluorescence was measured by flow cytometry on a BD LSRFortessa cytometer using BD FACSDiva Software (BD Biosciences) and Flowjo Software 10 (Flowjo LCC, Ashland, OR, USA). Ten thousand events were evaluated per experiment, and cellular debris was omitted from the analysis.

2.8. Morphological analysis

To evaluate alterations in morphology, cells were cultured under coverslips and stained with May-Grunwald-Giemsa. Morphological changes were examined by light microscopy using Image-Pro software. In addition, light scattering features were determined by flow cytometry as described above.

2.9. Annexin V/PI staining assay

For detection of apoptosis, we used a FITC Annexin V Apoptosis Detection Kit (BD Biosciences), according to the manufacturer's instructions. Cell fluorescence was determined by flow cytometry, as described above.

Protection assays using the pan-caspase inhibitor Z-VAD(Ome)-FMK (Cayman Chemical, Ann Arbor, MI, USA) and the antioxidant N-acetyl-l-cysteine (NAC) (Sigma-Aldrich Co.) were also performed. Briefly, the cells were pretreated for 2 h with 50 μM Z-VAD(Ome)-FMK or for 1 h with 5 mMNAC, and the pretreated cells were then incubated with β-lapachone and its 3-iodine derivatives for 72 h. The treated cells were trypsinized, and FITC Annexin V Apoptosis Detection assays were conducted as described above.

2.10. Measurement of the mitochondrial membrane potential with rhodamine 123

Mitochondrial membrane potential was determined by retention of rhodamine 123. Briefly, HSC3 cells were treated with β-lapachone and its 3-iodine derivatives for 24 or 48 h. The cells were then incubated with rhodamine 123 (5 μg/mL; Sigma-Aldrich Co.) at 37 °C for 15 min in the dark and washed with saline. Finally, the cells were incubated in saline at 37 °C for 30 min in the dark, and cell fluorescence was determined by flow cytometry as described above.

2.11. Caspase-8 and -9 activation assays

A caspase-8 colorimetric assay kit (BioVision Inc., Milpitas, CA, USA) and a caspase-9 colorimetric assay kit (Invitrogen, Frederick, MD, USA) were used to investigate the activation of caspase-8 and -9 in HSC3 cells treated with β-lapachone and its 3-iodine derivatives. The analyses were performed according to the manufacturers' instructions.

2.12. Analysis of intracellular reactive oxygen species levels

Intracellular reactive oxygen species (ROS) production was determined using 2′,7′-dichlorofluorescin diacetate (DCF-DA; Sigma-Aldrich Co.). Briefly, HSC3 cells were treated with β-lapachone and its 3-iodine derivatives for 1 or 3 h. The cells were then collected, washed with saline, and resuspended in FACS tubes with saline containing 5 μM DCF-DA for 30 min. Finally, the cells were washed with saline, and the fluorescence was determined by flow cytometry as described above.

Additionally, protection assays using the antioxidants NAC (Sigma-Aldrich Co.) and catalase (Sigma-Aldrich Co.) were also performed. Briefly, the cells were incubated with 5 mM NAC or 2000 UI catalase for 1 h and then incubated with β-lapachone and its 3-iodine derivatives for 1 h.

2.13. Measurement of cellular superoxide anion levels

Hydroethidine (Sigma-Aldrich Co.) was used to detect cellular superoxide levels after 1 h of treatment with β-lapachone and its 3-iodine derivatives [29]. The cells were labeled with 10 μM hydroethidine for 30 min. Finally, the cells were washed with saline, and fluorescence was determined as described above.

2.14. Measurement of nitric oxide production

Nitric oxide generation was detected with 4-amino-5-methylamino-2′-,7′-difluofluorescein diacetate (DAF-FM diacetate; Molecular Probes, Eugene, OR, USA) after 1 h of treatment with β-lapachone and its 3-iodine derivatives [30]. The cells were labeled with 3 μM DAF-FM diacetate for 60 min at 37 °C. Following staining, cells were washed with saline and incubated for an additional 15 min at 37 °C to allow for complete deesterification of the intracellular diacatates. The nitric oxide radical was then detected by flow cytometry as described above.

2.15. DNA intercalation assay

DNA intercalation was assessed by examining the ability of the compounds to displace ethidium bromide from calf thymus DNA (ctDNA) (Sigma-Aldrich Co.) [31]. Sextuplicate assays (100 μL) were conducted in 96-well plates and contained 15 μg/mL ctDNA, 1.5 μM ethidium bromide, and 5, 10, or 20 μM β-lapachone and its 3-iodine derivatives in 100 μL saline solution. The vehicle (0.2% dimethyl sulfoxide [DMSO]) used for diluting the compounds was also used as the negative control. Doxorubicin (20 μM) was used as the positive control. Fluorescence was measured using excitation and emission wavelengths of 320 and 600 nm, respectively, on a spectraMax Microplate Reader (Molecular Devices).

2.16. Gene expression analysis using a quantitative polymerase chain reaction (qPCR) array

HSC3 cells were plated in tissue culture bottles (7×10^4 cells/mL). After 12 h of incubation with 1 μM β-lapachone, 9 μM 3-I-α-lapachone, or 2 μM 3-I-β-lapachone, total RNA was isolated from the cells using an RNeasy Plus mini kit (Qiagen, Hilden, Germany) according to the manufacturer's instructions. The RNA was evaluated by fluorimetry (QuBit; Life Technologies, Camarillo, CA, USA). RNA reverse transcription was performed using Superscript VILO (Invitrogen

Table 1
Cytotoxic activity of β-lapachone and its 3-iodine derivatives.

Cells	IC_{50} in μM			
	DOX	β-lapachone	3-I-α-lapachone	3-I-β-lapachone
Cancer cells				
HSC3	0.34	1.02	4.39	0.98
	0.05–0.66	0.70–1.52	3.13–6.19	0.70–1.40
SCC4	0.07	16.22	7.47	1.84
	0.05–0.09	10.70–25.06	6.31–9.11	1.40–2.1
SCC9	0.77	0.16	8.43	2.50
	0.14–1.26	0.03–0.56	5.42–13.15	1.17–5.61
SCC15	1.49	0.06	4.34	0.81
	0.42–1.57	0.03–1.29	3.11–6.07	0.47–1.64
SCC25	1.40	2.78	8.08	2.50
	0.61–2.92	2.05–3.74	6.50–10.04	2.10–3.04
HepG2	0.01	0.99	11.77	0.44
	0.01–0.04	0.50–1.95	9.44–14.65	0.23–0.93
HL-60	0.01	0.09	4.04	0.02
	0.01–0.03	0.03–0.60	3.22–5.07	0.02–0.12
K562	0.05	1.35	2.17	0.74
	0.04–0.09	0.36–2.22	0.77–5.47	0.23–1.64
AGP-01	1.89	20.33	8.43	0.72
	0.45–2.34	14.77–27.98	6.82–10.40	0.23–1.64
ACP-02	6.82	48.94	11.30	1.40
	0.56–24.31	34.17–70.13	9.70–13.15	1.17–1.64
ACP-03	2.35	15.49	4.79	0.74
	0.51–3.20	10.76–22.28	3.57–6.40	0.47–1.17
HT-29	0.27	25.03	6.61	1.12
	0.26–0.44	18.14–34.60	5.34–7.90	0.93–1.40
HCT-116	0.18	5.62	3.03	0.44
	0.12–0.42	4.67–6.75	2.52–3.67	0.23–0.47
Non cancer cells				
HaCaT	0.11	0.43	8.01	1.82
	0.01–0.30	0.10–1.95	4.44–14.46	0.93–3.55
MRC5	0.82	37.71	4.32	1.25
	0.48–1.25	19.67–72.18	4.26–5.72	0.77–1.87
PBMC	5.17	82.78	14.79	33.69
	1.39–5.67	53.7–90.8	5.02–18.62	12.54–38.70

Data are presented as IC_{50} values in μM and their respective 95% confidence interval obtained by nonlinear regression from at the least three independent experiments performed in duplicate, measured by alamar blue assay after 72 h incubation. Cancer cells: HSC3 (human oral squamous cell carcinoma); SCC4 (human oral squamous cell carcinoma); SCC9 (human oral squamous cell carcinoma); SCC15 (human oral squamous cell carcinoma); SCC25 (human oral squamous cell carcinoma); HepG2 (human hepatocellular carcinoma); HL-60 (human promyelocytic leukemia); K562 (human chronic myelogenous leukemia); AGP-01 (human ascitic gastric adenocarcinoma); ACP-02 (human gastric adenocarcinoma); ACP-03 (human gastric adenocarcinoma); HT-29 (human colon adenocarcinoma) and HCT-116 (human colon carcinoma). Non-cancer cells: MRC5 (human lung fibroblast), HaCaT (human keratinocyte) and PBMC (human peripheral blood mononuclear cells). Doxorubicin (DOX) was used as positive control.

Corporation, Waltham, MA, USA). TaqMan Array Human Molecular Mechanisms of Cancer 96-well plates (ID 4418806; Applied Biosystems, Foster City, CA, USA) were used for gene expression analysis with qPCR. The reactions were conducted on an ABI ViiA7 instrument (Applied Biosystems). The cycle conditions included 2 min at 50 °C, 20 s at 95 °C, and 40 cycles of 3 s at 95 °C and 30 s at 60 °C. The relative quantification (RQ) of mRNA expression was calculated by the $2^{-\Delta\Delta CT}$ method using Gene Expression Suite Software (Applied Biosystems), and cells treated with the negative control (0.2% DMSO) were used as a calibrator. The *GAPDH*, *18S*, and *HPRT1* genes were used for normalization. All experiments were performed under DNase/RNase-free conditions. The genes were considered to be upregulated if the RQ was greater than or equal to 2 and downregulated if the RQ was less than or equal to 0.5.

2.17. In vivo study with OSCC xenografts

In total, 118 C.B-17 SCID mice (female, 25–30 g) were obtained and maintained at the animal facilities of Gonçalo Moniz Institute-FIOCRUZ (Salvador, Bahia, Brazil). Animals were housed in cages with free access to food and water. All animals were kept under a 12:12-h light/dark cycle (lights on at 6:00 a.m.). The local Animal Ethics Committee approved the experimental protocol (Approval number 06/2015).

In vivo antitumor efficacy was evaluated in a heterotopic xenograft model by inoculation of mice with HSC3 cells (1×10^7 cells/500 μL/animal) implanted subcutaneously in the left axilla of the mice. The compounds were dissolved in 5% DMSO and diluted in distilled water. The treatment was started 72 h after inoculation and was performed intraperitoneally once daily for 27 consecutive days. The mice were divided into seven groups, as follows: negative control group, animals treated with the vehicle (5% DMSO); positive control group, animals treated with doxorubicin (0.1 mg/kg); and experimental groups, animals treated with β-lapachone (20 mg/kg), 3-I-α-lapachone (20 or 40 mg/kg), or 3-I-β-lapachone (20 or 40 mg/kg). At the end of the treatment, peripheral blood samples from the mice were collected from the retro-orbital plexus for biochemical and hematological analysis after anesthesia, as described below. The animals were then euthanized by anesthesia overdose. The tumors were excised and weighed, as were the liver, lungs, heart, and kidneys of the mice. The effects of the compounds were expressed as percent inhibition relative to the control.

2.18. Toxicological evaluation

Mice were weighed at the beginning and at the end of the experiment. In addition, the animals were observed for signs of changes throughout the study. The liver, kidneys, heart, and lungs were removed, weighed, and observed for any signs of severe injury or changes in color and bleeding.

Hematological analyses were performed by light microscopy. Hematological parameters, including total erythrocyte and leukocyte counts, as well as differential counts of leukocytes, such as neutrophils, lymphocytes, monocytes, eosinophils, and basophils, were quantified.

Biochemical analyses of serum samples were performed using a Vet-16 rotor (Hemagen Diagnostics Inc., Columbia, MD, USA). Glutamic-oxalacetic transaminase, glutamic-pyruvic transaminase, amylase, nitrogen urea, glucose, phosphorus, calcium, uric acid, creatine kinase, total proteins, and globulin were analyzed.

After fixation in 4% formaldehyde, tumors, livers, kidneys, hearts, and lungs were examined for size, color, and hemorrhage. Histological analyses were performed under optical microscopy using hematoxylin-eosin and Periodic acid-Schiff (liver and kidney) staining, by an experienced pathologist.

2.19. Statistical analysis

The results were compiled into a database organized in spreadsheets in Microsoft Excel, and statistical analysis was performed using GraphPad Prism. The data were analyzed according to the distribution in the normal Gaussian curve. The half-maximal inhibitory concentration (IC_{50}) values were obtained by nonlinear regression from three independent experiments performed in duplicate. The differences between groups were evaluated by analysis of variance followed by Student-Newman-Keuls tests ($p < 0.05$).

For gene expression analysis, after amplification and dissociation runs, the relative quantity values were obtained with the aid of the Gene Expression Suite program (Applied Biosystems) according to the comparative Cq method (ΔΔCQ) [32].

3. Results

3.1. β-Lapachone and its 3-iodine derivatives exhibited potent cytotoxicity against a panel of human cancer cell lines

The cytotoxic effects of β-lapachone and its 3-iodine derivatives were assessed in different human cancer cell lines using Alamar Blue assays after 72 h of incubation. Table 1 shows the IC_{50} values obtained from this analysis. β-Lapachone showed cytotoxicity with IC_{50} values ranging from 0.06 to 48.9 μM for SCC15 and APC02 cells, respectively. Additionally, 3-I-α-lapachone had IC_{50} values ranging from 2.2 to 11.8 μM for K562 and HepG2 cells, respectively, whereas 3-I-β-lapachone had IC_{50} values ranging from 0.02 to 2.5 μM for HL-60 and SCC9/SCC25 cells, respectively. Interestingly, 3-I-α-lapachone showed more potent cytotoxicity than β-lapachone in SCC4 (2-fold), AGP-01 (2.4-fold), ACP-02 (4.3-fold), ACP-03 (3.2-fold), and HT-29 (3.8-fold) cells. In contrast, 3-I-β-lapachone showed more potent cytotoxicity than β-lapachone in SCC4 (9-fold), HepG2 (2.5-fold), AGP-01 (29-fold), ACP-02 (35-fold), ACP-03 (22-fold), HCT-29 (27-fold), and HCT-116 (14-fold) cells.

In HaCaT cells, MRC5 cells, and PBMCs, as representative noncancer cell lines, β-lapachone showed IC_{50} values of 0.4, 37.7, and 82.7 μM, respectively; 3-I-α-lapachone showed IC_{50} values of 8.0, 4.3, and 14.8 μM, respectively; and 3-I-β-lapachone showed IC_{50} values of 1.8, 1.2, and 33.8 μM, respectively. The results for the selectivity index (SI) analysis are shown in Table 2. β-Lapachone and its 3-iodine derivatives showed greater selectivity of cytotoxicity for cancer cells than PBMCs. In HSC3 cells, β-lapachone, 3-I-α-lapachone, and 3-I-β-lapachone showed SIs of 82.7, 3.3, and 33.8, respectively, and doxorubicin, which was used as a positive control, also showed cytotoxic activity, with IC_{50} values ranging from 0.01 to 6.8 μM for HL-60/HepG2 and APC02 cells, respectively. In noncancer cells, doxorubicin exhibited IC_{50} values of 0.1, 0.8, and 5.2 μM for HaCaT cells, MRC5 cells, and PBMCs, respectively.

To study the cytotoxic potential of β-lapachone and its 3-iodine derivatives in OSCC cells, a new set of experiments was performed to evaluate the effects and mechanisms of action of these compounds in HSC3 cells, which showed high sensitivity to the compounds. The cytotoxic effects of β-lapachone and its 3-iodine derivatives were confirmed in vitro in a three-dimensional (3D) model of multicellular cancer spheroids. Fig. 2**a** shows the morphological alterations in spheroids treated with β-lapachone and its 3-iodine derivatives, indicating drug permeability in the 3D culture. The IC_{50} value of β-lapachone was 9.8 μM after 72 h of incubation (Fig. 2**b**), and 3-I-α-lapachone and 3-I-β-lapachone showed IC_{50} values of 8.1 and 2.3 μM, respectively. Doxorubicin presented an IC_{50} value of 43.5 μM.

Next, we performed the trypan blue exclusion assay to assess the effects of β-lapachone and its 3-iodine derivatives on cell viability after incubation for different times (Fig. S1). The results demonstrated that treatment with the compounds significantly reduced the number of viable cells compared with the negative control (0.2% DMSO) after 12, 24, 48, and 72 h of exposure. Doxorubicin also reduced the number of viable cells during the time course of treatment. There were no significant differences in the number of nonviable cells among groups.

Treatment with β-lapachone, its 3-iodine derivatives, and doxorubicin in HSC3 cells caused cell volume reduction, chromatin condensation, apoptotic bodies, and nuclear fragmentation, which became more evident at higher concentrations and after longer incubation times (Fig. S2). Furthermore, β-lapachone and its iodine derivatives caused cell shrinkage, as revealed by the decrease in forward light scatter, and nuclear condensation, as shown by a transient increase in side scatter, suggesting induction of apoptosis (Fig. S3).

3.2. β-Lapachone and its 3-iodine derivatives failed to induce DNA intercalation

β-Lapachone and its 3-iodine derivatives failed to induce DNA intercalation in ethidium bromide displacement assays using ctDNA (data not shown). In contrast, doxorubicin, a known DNA intercalator, was able to displace ethidium bromide from ctDNA.

3.3. β-Lapachone and its 3-iodine derivatives promoted G_2/M phase arrest and increased internucleosomal DNA fragmentation in HSC3 cells

Next, we measured the DNA content by flow cytometry to determinate the internucleosomal DNA fragmentation and cell cycle distribution. All DNA that was sub-diploid in size (sub-G_1) was considered fragmented, which can be used as an indicator of apoptosis when the cell membrane remain integrity. After 24 h of incubation, a significant increase in the percentage of HSC3 cells at G_2/M phase was observed

Table 2
Selectivity index of β-lapachone and its 3-iodine derivatives.

Cancer cells	Non-cancer cells											
	HaCaT				MRC5				PBMC			
	DOX	β-lap	3-I-α-lap	3-I-β-lap	DOX	β-lap	3-I-α-lap	3-I-β-lap	DOX	β-lap	3-I-α-lap	3-I-β-lap
HSC3	0.3	0.4	1.8	1.8	2.7	37.7	0.9	1.2	17.3	82.7	3.3	33.8
SCC4	1.4	0.02	1.1	1.0	11.4	2.3	0.6	0.7	74.3	5.1	2.0	18.8
SCC9	0.1	2.0	1.0	0.7	1.0	188.5	0.5	0.5	6.5	413.5	1.8	13.5
SCC15	0.07	6.7	1.9	2.3	0.5	628.3	1.0	1.5	3.5	1378.3	3.4	42.3
SCC25	0.07	0.1	1.0	0.7	0.6	13.4	0.5	0.5	3.7	29.5	1.8	13.5
HepG2	10.0	0.4	0.7	4.5	80.0	37.7	0.4	3.0	520.0	82.7	1.3	84.5
HL-60	10.0	4.0	2.0	90.0	80.0	377.0	1.1	60.0	520.0	827.0	3.7	1690.0
K562	2.0	0.3	3.6	2.6	16.0	29.0	1.9	1.7	104.0	63.6	6.7	48.3
AGP-01	0.05	0.02	1.0	2.6	0.4	1.8	0.5	1.7	2.7	4.1	1.8	48.3
ACP-02	0.01	0.01	0.8	1.3	0.1	0.8	0.4	0.8	0.7	1.7	1.3	24.1
ACP-03	0.04	0.03	1.6	2.6	0.3	2.4	0.9	1.7	2.3	5.3	3.1	48.3
HT-29	0.3	0.02	1.2	1.6	2.7	1.6	0.6	1.9	17.3	3.3	2.2	30.7
HCT-116	0.5	0.07	2.7	4.5	4.0	6.8	1.4	3.0	26.0	14.8	4.9	84.5

Data are presented as the selectivity index (SI) calculated using the following formula: SI = IC_{50}[non-cancer cells]/IC_{50}[cancer cells]. Cancer cells: HSC3 (human oral squamous cell carcinoma); SCC4 (human oral squamous cell carcinoma); SCC9 (human oral squamous cell carcinoma); SCC15 (human oral squamous cell carcinoma); SCC25 (human oral squamous cell carcinoma); HepG2 (human hepatocellular carcinoma); HL-60 (human promyelocytic leukemia); K562 (human chronic myelogenous leukemia); AGP-01 (human ascitic gastric adenocarcinoma); ACP-02 (human gastric adenocarcinoma); ACP-03 (human gastric adenocarcinoma); HT-29 (human colon adenocarcinoma) and HCT-116 (human colon carcinoma). Non-cancer cells: MRC5 (human lung fibroblast), HaCaT (human keratinocyte) and PBMC (human peripheral blood mononuclear cells). Doxorubicin (DOX) was used as positive control.

A

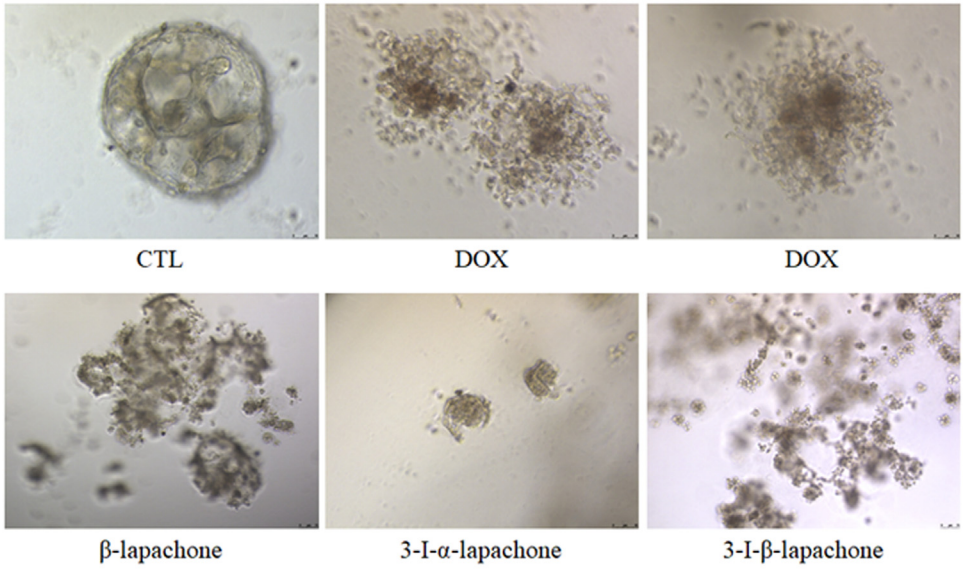

B

Spheroids	IC_{50} in μM			
	DOX	β-lapachone	3-I-α-lapachone	3-I-β-lapachone
HSC3	43.5	9.8	8.1	2.3
	22.4 – 84.6	5.6 – 16.9	4.9 – 13.3	1.5 – 3.6

Fig. 2. Effects of the β-lapachone and its 3-iodine derivatives in 3D in vitro model of cancer multicellular spheroids formed from HSC3 cells. a. Cells in the 3D in vitro model examined by light microscopy. **b**. IC_{50} values, in μM, and their respective 95% confidence interval obtained by nonlinear regression from at the least three independent experiments performed in duplicate, measured by alamar blue assay after 72 h of incubation. The negative control (CTL) was treated with the vehicle (0.5% DMSO) used for diluting the compounds tested. Doxorubicin (DOX) was used as the positive control.

Table 3
Effect of β-lapachone and its 3-iodine derivatives in the cell cycle distribution of HSC3 cells.

Treatment	Concentration (μM)	DNA content (%)			
		Sub-G_0/G_1	G_0/G_1	S	G_2/M
After 12 h incubation					
CTL	–	2.8 ± 1.1	51.5 ± 3.7	11.5 ± 2.4	25.7 ± 1.0
DOX	0.5	8.0 ± 3.0	48.1 ± 9.2	9.7 ± 1.7	42.3 ± 7.2
β-lapachone	1	5.7 ± 1.6	32.0 ± 4.0*	21.9 ± 3.9*	37.5 ± 6.2
3-I-α-lapachone	4.5	8.4 ± 3.0	36.2 ± 2.6	24.8 ± 3.3*	27.8 ± 2.8
	9	8.1 ± 2.3	36.8 ± 1.1	25.8 ± 1.2*	30.2 ± 6.3
3-I-β-lapachone	1	7.7 ± 4.3	33.9 ± 3.8*	18.1 ± 1.1	34.5 ± 4.5
	2	14.9 ± 4.8	33.1 ± 1.8*	16.5 ± 3.3	29.2 ± 5.2
After 24 h incubation					
CTL	–	5.2 ± 0.8	55.0 ± 3.3	16.4 ± 1.6	20.0 ± 1.9
DOX	0.5	18.9 ± 1.9	31.8 ± 2.9*	10.9 ± 1.5	37.2 ± 4.1*
β-lapachone	1	4.6 ± 10	33.0 ± 6.2*	17.3 ± 3.0	40.6 ± 5.7*
3-I-α-lapachone	4.5	8.3 ± 2.3	42.0 ± 4.5	16.0 ± 1.2	32.2 ± 3.7
	9	8.7 ± 1.4	33.1 ± 6.3*	16.6 ± 3.8	41.5 ± 3.9*
3-I-β-lapachone	1	9.2 ± 2.9	41.8 ± 2.5	14.1 ± 2.8	33.5 ± 3.7
	2	27.1 ± 9.8*	38.2 ± 6.5	13.3 ± 2.9	21.1 ± 2.0
After 48 h incubation					
CTL	–	10.6 ± 1.7	56.1 ± 5.2	14.3 ± 2.3	13.7 ± 1.4
DOX	0.5	65.7 ± 3.3*	14.4 ± 2.5*	5.7 ± 1.7*	8.8 ± 1.1
β-lapachone	1	25.6 ± 4.5	38.1 ± 4.1*	12.2 ± 3.1	23.7 ± 4.0
3-I-α-lapachone	4.5	15.9 ± 1.4	49.8 ± 2.6	10.3 ± 1.6	18.9 ± 2.5
	9	18.8 ± 1.5	47.6 ± 3.0	9.7 ± 1.4	23.2 ± 3.8
3-I-β-lapachone	1	32.3 ± 10.1*	38.9 ± 5.5*	8.0 ± 1.6	20.6 ± 4.5
	2	80.8 ± 5.5*	11.6 ± 4.3*	2.9 ± 1.0*	4.7 ± 1.5
After 72 h incubation					
CTL	–	17.3 ± 1.7	62.4 ± 6.0	7.6 ± 0.9	10.3 ± 2.6
DOX	0.5	69.5 ± 10.1*	12.9 ± 4.3*	4.9 ± 1.6	13.8 ± 4.9
β-lapachone	1	22.4 ± 1.5	39.3 ± 5.1*	10.4 ± 2.2	29.1 ± 2.5*
3-I-α-lapachone	4.5	26.0 ± 4.1	44.6 ± 5.2*	8.1 ± 2.1	20.3 ± 8.0
	9	27.3 ± 3.1	40.3 ± 3.9*	10.3 ± 1.9	19.0 ± 2.8
3-I-β-lapachone	1	34.7 ± 3.2	39.1 ± 4.3*	11.0 ± 1.9	13.6 ± 1.5
	2	80.8 ± 6.3*	12.7 ± 4.6*	2.0 ± 0.5	4.3 ± 1.4

Data are presented as the mean ± S.E.M. of three independent experiments performed in duplicate. The negative control (CTL) was treated with the vehicle (0.2% DMSO) used for diluting the compounds tested. Doxorubicin (DOX) was used as positive control. Ten thousand events were evaluated per experiment and cellular debris were omitted from the analysis. * $p < 0.05$ compared with the negative control by ANOVA followed by Student Newman-Keuls Test.

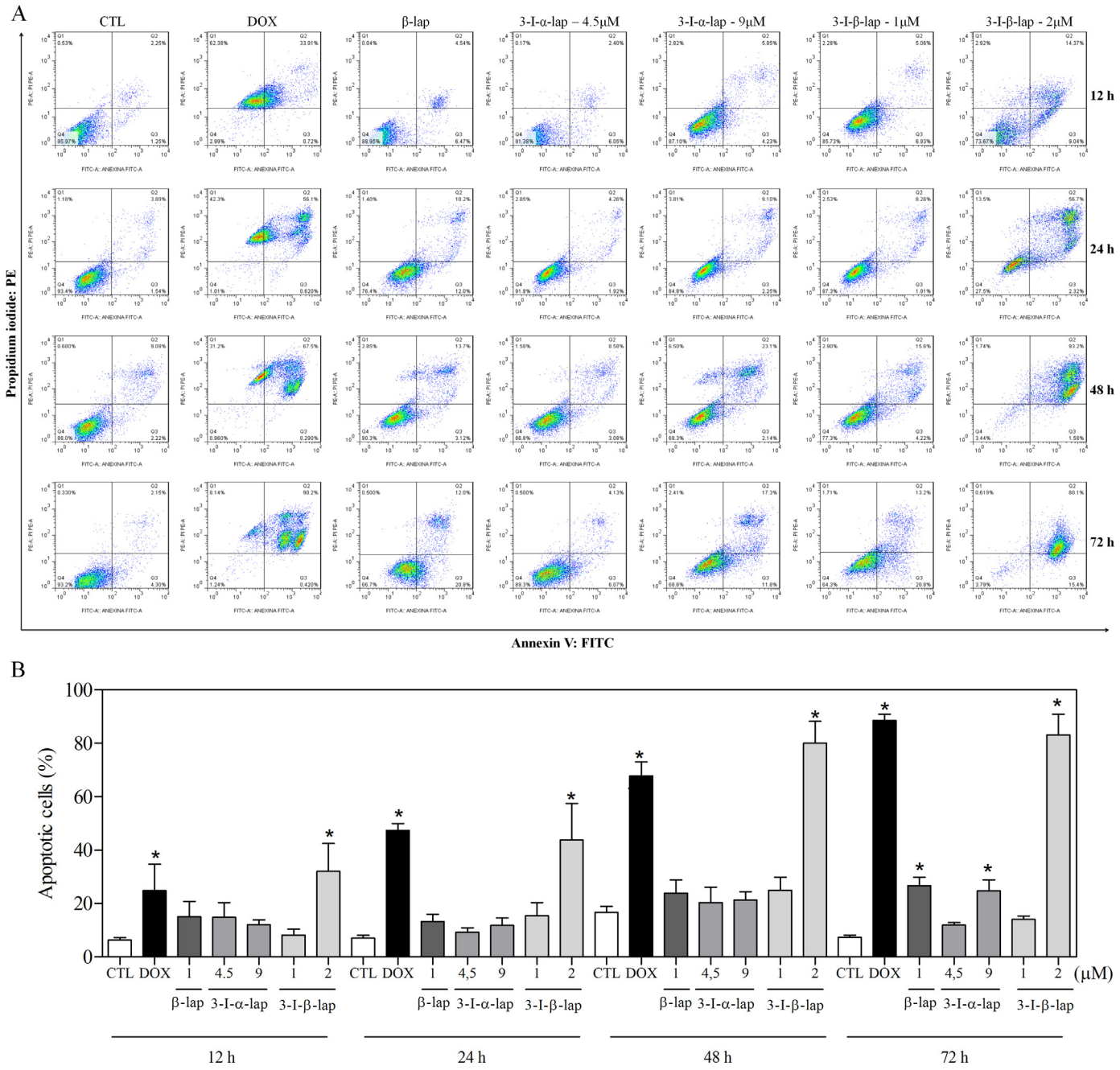

Fig. 3. Effects of the β-lapachone and its 3-iodine derivatives on the induction of apoptosis in HSC3 cells after 12, 24, 48 and 72 h of incubation, as determined by flow cytometry using annexin V-FITC/PI staining. a. Representative flow cytometry dot plots show the percent cells in the viable, early apoptotic, late apoptotic and necrotic stages. **b**. Quantification of apoptotic HSC3 cells. The negative control (CTL) was treated with the vehicle (0.2% DMSO) used for diluting the compounds tested. Doxorubicin (DOX, 0.5 μM) was used as positive control. Data are presented as the means ± S.E.M. of three independent experiments performed in duplicate. Ten thousand events were evaluated per experiment and cellular debris were omitted from the analysis. * $p < 0.05$ compared with the negative control by ANOVA, followed by the Student–Newman–Keuls test.

(40.6% for treatment with β-lapachone at 1 μM, and 41.5% for treatment with 3-iodine-α-lapachone at 9 μM, compared with 20.0% for the negative control; Table 3). Cell cycle arrest at the G_2/M phase was followed by an increase in internucleosomal DNA fragmentation, as observed after 48 or 72 h of incubation with 3-iodine-β-lapachone. Doxorubicin induced cell cycle arrest at G_2/M phase within 24 h of incubation. After 48 h of incubation, the treatment increased internucleosomal DNA fragmentation, as observed by the significant increase in the number of cells in sub-G_1 (Table 3).

3.4. β-Lapachone and its 3-iodine derivatives induced caspase- and mitochondria-dependent apoptosis in HSC3 cells

Evaluation of cell death profiles was verified by the externalization of phosphatidylserine and permeability of the cytoplasmic membrane using annexin V-fluorescein isothiocyanate (FITC) and propidium iodide (PI) staining (Fig. 3). The results demonstrated significant exposure of phosphatidylserine in HSC3 cells treated with 2 μM 3-I-β-lapachone, at all time points, when compared with the negative control group (0.2% DMSO). β-Lapachone and 3-I-α-lapachone showed significant phosphatidylserine exposure only after 72 h of incubation.

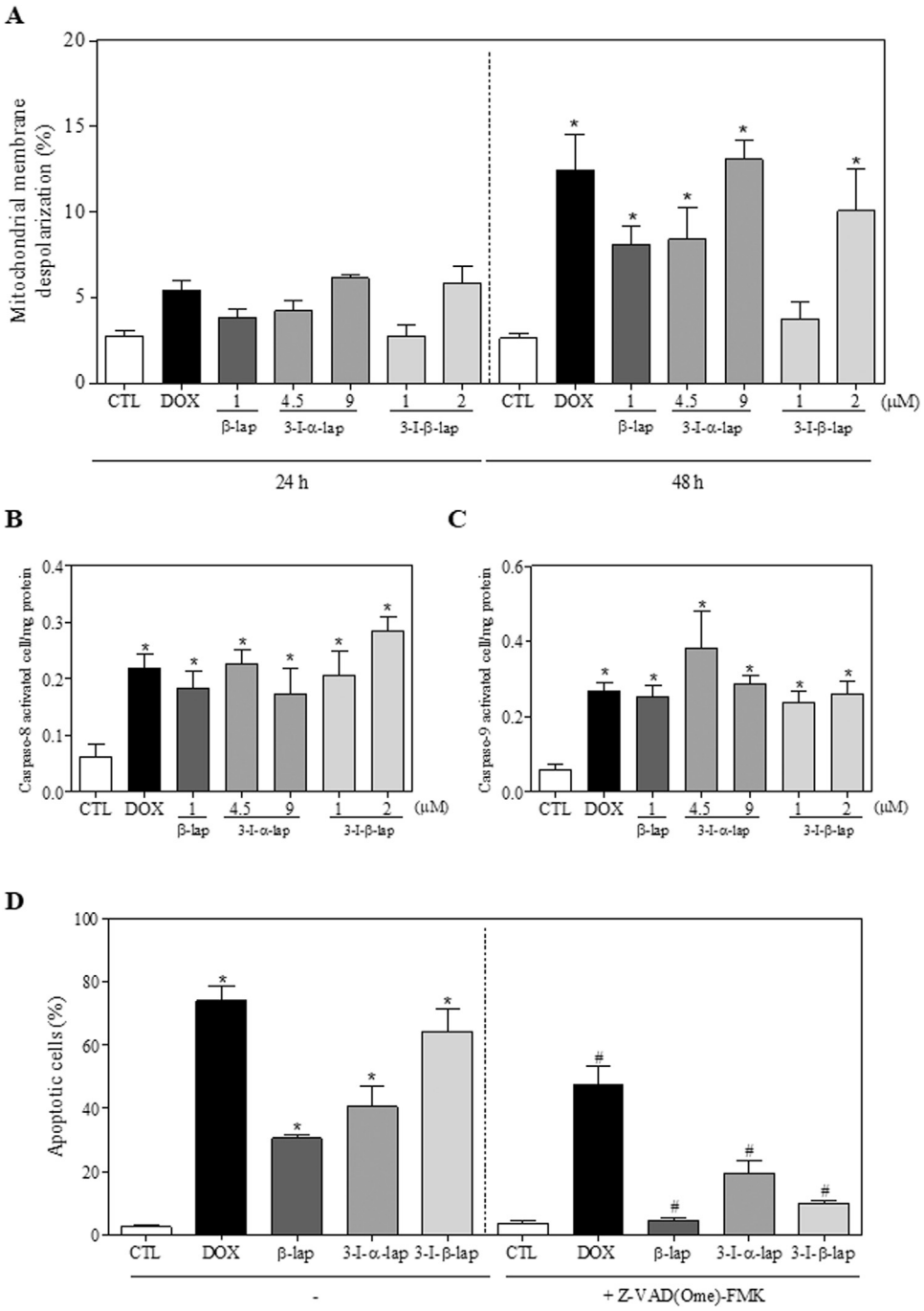

Fig. 4. Effects of the β-lapachone and its 3-iodine derivatives on the mitochondrial membrane potential, caspase-8 and 9 activity and effects of pan-caspase (Z-VAD (Ome)-FMK) inhibitor in the apoptosis induced by the compounds in HSC3 cells. a. Mitochondrial membrane potential determined by flow cytometry using rhodamine 123 staining after 24 and 48 h of incubation. **b**. Caspase-8 activity determined by colorimetric assay after 72 h of incubation. **c**. Caspase-9 activity determined by colorimetric assay after 72 h of incubation. **d**. Effects of pan-caspase (Z-VAD(Ome)-FMK) inhibitors in the apoptosis induced by β-lapachone and its 3-iodine derivatives in HSC3 cells after 72 h of incubation, determined by flow cytometry using annexin V-FITC/PI. For the protection assay, the cells were pretreated for 2 h with 50 μM Z-VAD (Ome)-FMK and then incubated with 1 μM β-lapachone, 9 μM 3-I-α-lapachone and 1 μM 3-I-β-lapachone for 72 h. The negative control (CTL) was treated with the vehicle (0.2% DMSO) used for diluting the compounds tested. Doxorubicin (DOX, 0.5 μM) was used as positive control. Data are presented as the means ± S.E.M. of three independent experiments performed in duplicate. For flow cytometry analysis, 10,000 events were evaluated per experiment and cellular debris was omitted from the analysis. * $p < 0.05$ compared with the negative control by ANOVA, followed by the Student–Newman–Keuls test. # $p < 0.05$ compared with the respective treatment without inhibitor by ANOVA followed by Student Newman-Keuls test.

Doxorubicin, used as a positive control, induced a significant increase in phosphatidylserine externalization at all time points when compared with the negative control group (0.2% DMSO). An increase in PI-only labeling was also observed in doxorubicin-treated cells, indicating membrane damage without external exposure of phosphatidylserine.

β-Lapachone and its 3-iodine derivatives induced mitochondrial depolarization in HSC3 cells 48 h after treatment, as measured by incorporation of rhodamine 123 using flow cytometry (Fig. 4**a**). Additionally, a significant increase in the activation of caspase-8 and -9 in HSC3 cells treated with β-lapachone and its 3-iodine derivatives was observed (Fig. 4**b and c**). Moreover, treatment with the positive control (doxorubicin) induced significant activation of caspase-8 and -9, and cotreatment with the pan-caspase inhibitor Z-VAD(OMe)-FMK attenuated the effects of the compounds on apoptosis (Fig. 4**d** and S4).

The cytotoxic activity of β-lapachone and its 3-iodine derivatives was evaluated in murine immortalized embryonic fibroblasts isolated from *Bad* -knockout mice (BAD-KO SV40 MEFs). As a control, wild-type embryonic fibroblasts (WT SV40 MEFs) were used. The IC_{50} values for β-lapachone were 0.7 and 0.5 μM for WT SV40 MEFs and BAD-KO SV40 MEFs, respectively; those for 3-I-α-lapachone were 5.1 and 3.5 μM in WT SV40 MEFs and BAD-KO SV40 MEFs, respectively; and those for 3-I-β-lapachone were 4.0 and 1.7 μM for WT SV40 MEFs and BAD-KO SV40 MEFs, respectively. Cells treated with doxorubicin showed IC_{50} values of 0.04 and 0.41 μM in WT SV40 MEFs and BAD-KO SV40 MEFs, respectively.

3.5. β-Lapachone and its 3-iodine derivatives increase reactive oxygen species levels in HSC3 cells

Treatment with β-lapachone and its 3-iodine derivatives for 1 h

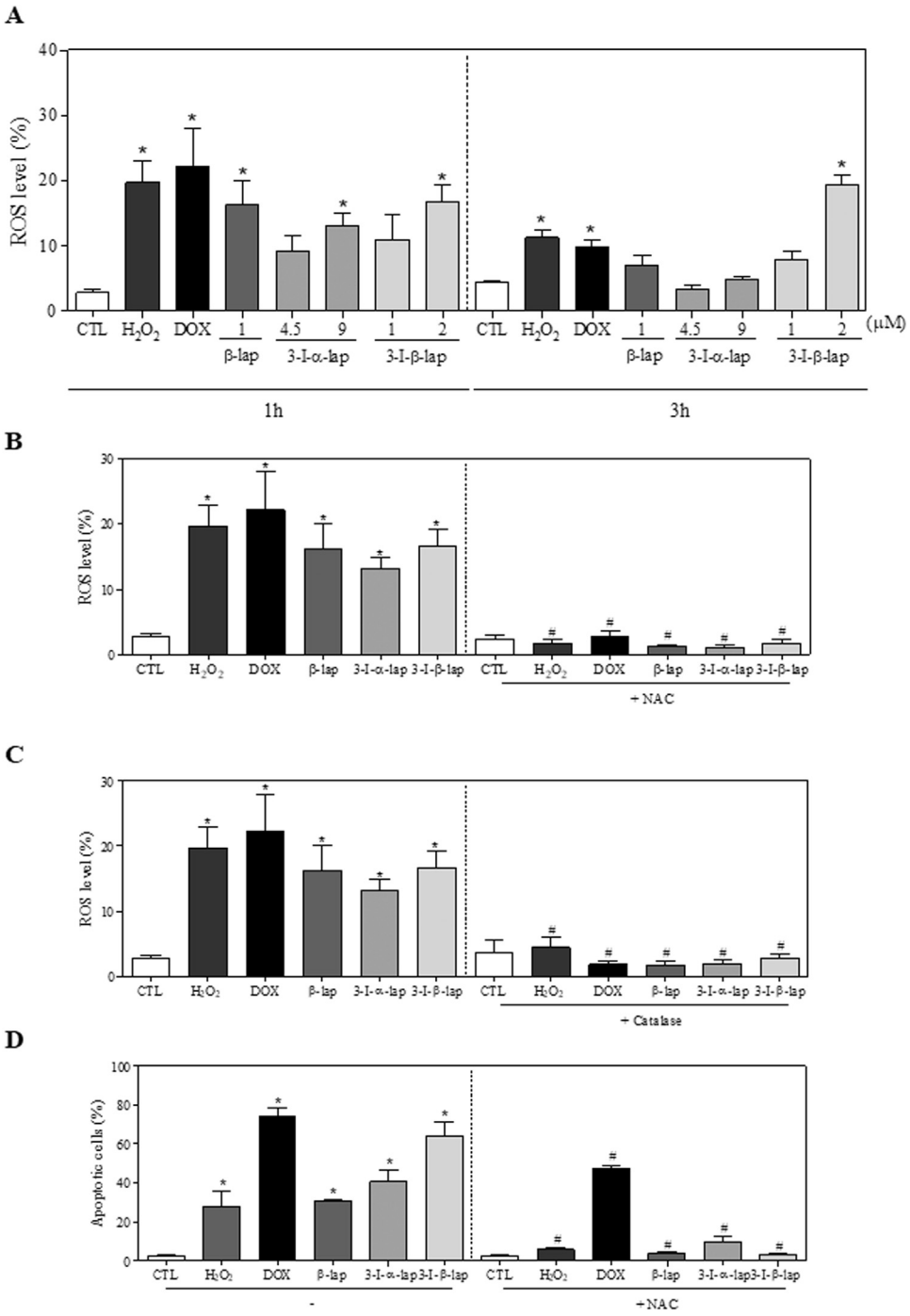

Fig. 5. Effects of β-lapachone and its 3-iodine derivatives in the levels of reactive oxygen species (ROS) of HSC3 cells and protection by N-acetyl-L-cysteine (NAC) and catalase, determined by flow cytometry. a. ROS levels of HSC3 cells after 1 and 3 h incubation using DCF-DA staining. **b**. ROS levels of HSC3 cells pre-treated with the antioxidant NAC, then treated with the compounds. **c**. ROS levels of HSC3 cells pre-treated with the antioxidant catalase, then treated with the compounds. For the protection assay, the cells were pre-treated for 1 h with 5 mM NAC or 2,000UI catalase, then incubated with the compounds for 1 h. d. Effects of NAC in the apoptosis induced by β-lapachone and its 3-iodine derivatives in HSC3 cells, determined by flow cytometry using annexin V-FITC/PI. For the protection assay, the cells were pre-treated for 1 h with 5 mM NAC and then incubated with 1 μM β-lapachone, 9 μM 3-I-α-lapachone and 1 μM 3-I-β-lapachone for 72 h. The negative control (CTL) was treated with the vehicle (0.2% of DMSO) used for diluting the compounds tested. Hydrogen peroxide (H_2O_2, 200 μM) and doxorubicin (DOX, 0.5 μM) were used as positive controls. Data are presented as the mean ± S.E.M. of three independent experiments performed in duplicate or triplicate. Ten thousand events were evaluated per experiment and cellular debris were omitted from the analysis. * $p < 0.05$ compared with the negative control by ANOVA followed by Student Newman-Keuls test. # $p < 0.05$ compared with the respective treatment without inhibitor by ANOVA followed by Student Newman-Keuls test.

caused a marked increase in ROS levels (Fig. 5**a**). In addition, cotreatment with the antioxidant NAC fully prevented the increase in intracellular ROS levels induced by β-lapachone and its 3-iodine derivatives (Fig. 5**b**). Moreover, cotreatment with catalase, which induces of hydrogen peroxide decomposition, prevented the increase in intracellular ROS level after treatment with the compounds, indicating the induction of hydrogen peroxide production by treatment with β-lapachone and its 3-iodine derivatives (Fig. 5**c**). Importantly, cotreatment with NAC prevented the increase in the cell death by apoptosis induced by β-lapachone and its 3-iodine derivatives (Fig. 5**d** and S5).

In a new set of experiments using fluorescent probes specific for individual species of ROS, the compounds were not able to produce intracellular superoxide anion (Fig. S6a). In contrast, addition of doxorubicin and hydrogen peroxide, used as positive controls, caused significant increases in superoxide anion levels in HSC3 cells 1 h after incubation. Fig. S6b shows the results of nitric oxide production after 1 h of treatment with β-lapachone and its 3-iodine derivatives in HSC3 cells, in which significant increases in nitric oxide levels were observed after 1 h for cells treated with 9 μM 3-I-α-lapachone, but not with the other compounds tested.

3.6. β-Lapachone and its 3-iodine derivatives altered gene expression in HSC3 cells

In total, 92 genes were investigated in HSC3 cells treated with β-lapachone and its 3-iodine derivatives for 12 h (Table 4). The expression was up-regulated on 44 genes for β-lapachone, 79 for 3-I-β-lapachone, 10 genes for 3-I-α-lapachone and 72 genes for doxorubicin.

Table 4
Effect β-lapachone and its 3-iodine derivatives on gene expression of HSC3 cells.

Genes	DOX	β-lapachone	3-I-α-lapachone	3-I-β-lapachone
ABL1	364.4	1.5	0.7	10.7
AKT1	570.9	3.6	1.3	42.9
AKT2	211.0	1.5	0.7	17.1
APC	356.3	2.1	0.7	69.8
BAX	1346.1	3.2	0.8	37.8
BCAR1	658.9	4.0	2.6	90.5
BCL2	372.3	N.d.	1.5	14.8
BCL2L1	263.9	1.4	0.6	12.3
BCL2L11	3037.1	4.7	1.7	27.0
BID	N.d.	0.9	2.9	3.9
BRAF	147.4	1.7	1.4	48.3
CASP8	40.1	0.9	0.7	4.9
CASP9	N.d.	1.6	N.d.	104.9
CCND1	1645.5	4.3	1.4	41.3
CCND2	658.4	2.6	0.6	25.8
CCND3	1382.3	11.6	1.5	42.1
CCNE1	1776.4	12.8	1.5	41.6
CDC42	N.d.	0.8	0.8	6.2
CDH1	318.8	2.4	1.3	21.0
CDK2	1826.0	5.0	0.6	32.3
CDK4	383.9	2.6	1.0	22.4
CDKN1A	4302.5	8.0	2.8	80.8
CDKN1B	335.8	1.6	0.6	22.4
CDKN2A	12.8	1.5	1.1	10.0
CDKN2B	N.d.	N.d.	N.d.	N.d.
COL1A1	1624.5	5.6	1.5	19.2
CRK	N.d.	0.9	1.4	3.0
CTNNB1	45.1	2.5	1.2	12.3
CYCS	N.d.	1.0	1.3	N.d.
DVL1	246.7	4.3	1.9	72.0
E2F1	1744.0	5.6	1.1	44.1
EGFR	121.2	2.2	0.9	42.0
ELK1	12.4	1.4	1.1	12.5
ERBB2	1748.6	4.7	1.4	64.2
FADD	N.d.	0.8	1.5	9.9
FAS	34.2	0.8	0.9	4.2
FASLG	N.d.	N.d.	N.d.	N.d.
FGF2	228.3	1.5	1.7	22.7
FN1	911.1	1.7	1.0	19.4
FOS	1065.4	1.8	1.7	27.0
FYN	99.8	1.1	0.9	23.0
FZD1	1221.6	5.5	1.0	47.9
GRB2	297.1	1.2	0.6	20.8
GSK3B	63.6	1.3	0.6	14.1
HGF	N.d.	N.d.	N.d.	N.d.
HRAS	392.2	3.0	1.1	28.1
IGF1	N.d.	N.d.	N.d.	N.d.
IGF1R	1398.5	3.5	0.7	22.1
ITGA2B	N.d.	N.d.	N.d.	N.d.
ITGAV	497.3	2.8	1.0	24.2
ITGB1	449.1	1.7	0.8	19.4
ITGB3	N.d.	N.d.	N.d.	N.d.
JUN	6603.6	4.5	1.9	51.8
KDR	N.d.	N.d.	N.d.	N.d.
KIT	N.d.	N.d.	N.d.	N.d.
KRAS	N.d.	2.7	2.9	13.3
LEF1	371.2	2.1	1.1	13.3
MAP2K1	18.7	1.4	1.3	20.2
MAP3K5	0.8	1.4	N.d.	0.8
MAPK	353.2	2.1	1.1	23.9
MAPK14	243.9	2.8	1.6	39.8
MAPK3	545.6	5.3	1.2	25.7
MAPK8	682.4	3.2	0.8	37.7
MAX	N.d.	N.d.	N.d.	N.d.
MDM2	466.6	2.5	1.2	36.6
MYC	662.5	1.7	0.7	26.0
NFKB1	536.3	3.0	0.7	11.7
NFKB2	1563.6	2.9	1.9	65.8
NFKBIA	782.3	2.3	1.6	36.5
NRAS	84.4	0.9	0.8	16.1
PIK3CA	210.2	0.7	0.8	22.1
PIK3R1	32.1	0.4	0.2	2.4
PTEN	N.d.	0.6	0.6	1.1
PTK2	381.3	2.7	1.3	37.0
PTK2B	651.0	2.8	0.9	42.5
RAC1	24.8	0.8	0.7	2.2
RAF1	140.0	0.8	0.6	9.6
RB1	269.1	2.0	1.1	16.2
RELA	383.3	2.3	0.8	20.4
RHOA	255.9	2.0	1.0	25.9
SHC1	3.7	1.4	2.1	5.3
SMAD4	151.5	1.4	0.8	19.3
SOS1	781.0	3.6	2.9	49.9
SPP1	N.d.	N.d.	13.3	89.9
SRC	904.0	3.6	1.7	52.8
TCF3	146.8	3.3	2.8	58.3
TGFB1	1930.2	4.8	1.1	52.2
TGFBR1	358.7	1.9	1.2	27.1
TGFBR2	330.9	0.1	0.8	55.4
TP53	95.5	2.5	2.9	2.8
VEGFA	605.9	1.7	2.8	50.5
WNT1	N.d.	N.d.	N.d.	N.d.

HSC3 cells were treated with 1 μM of β-lapachone, 4.5 μM of 3-I-α-lapachone and 1 μM of 3-I-β-lapachone for 12 h. The negative control was treated with the vehicle (0.2% DMSO) used for diluting the compound tested. Doxorubicin (DOX, 0.5 μM) was used as positive control. After treatment, total RNA was isolated and reverse transcribed. Gene expression was detected using the 96-well plate TaqMan® Array Human Molecular Mechanisms of Cancer. GAPDH, 18S and HPRT1 genes were used as endogenous genes for normalization. Values represent the relative quantitation (RQ) compared with the calibrator (cells treated with the negative control, RQ = 1.0). The genes were considered to be up-regulated if RQ ≥ 2 and were considered to be down-regulated if RQ ≤ 0.5. N.d. Not determined.

Downregulated genes was observed for only 2 genes for β-lapachone and for one gene for 3-I-α-lapachone (Table S2). Among the genes investigated, the pro-apoptotic genes *BAX* (relative quantification [RQ] = 3.2 for β-lapachone; RQ = 37.8 for 3-I-β-lapachone; RQ = 1346.1 for doxorubicin), *BCL2L11* (RQ = 4.7 for β-lapachone; RQ = 27.0 for 3-I-β-lapachone; RQ = 3037.1 for doxorubicin), and *E2F1* (RQ = 5.6 for β-lapachone; RQ = 44.1 for 3-I-β-lapachone; RQ = 1744.0 for doxorubicin) were upregulated. Additionally, the cell cycle control (G_1/S transition)-related genes *CCND1* (RQ = 4.3 for β-lapachone; RQ = 41.3 for 3-I-β-lapachone; RQ = 1645.5 for doxorubicin), *CCND3* (RQ = 11.6 for β-lapachone; RQ = 42.1 for 3-I-β-lapachone; RQ = 1382.3 for doxorubicin), *CCNE1* (RQ = 12.8 for β-lapachone; RQ = 41.6 for 3-I-β-lapachone; RQ = 1776.4 for doxorubicin), *CDK2* (RQ = 5.0 for β-lapachone; RQ = 32.3 for 3-I-β-lapachone; RQ = 1826.0 for doxorubicin), and *CDKN1A* (RQ = 8.0 for β-lapachone; RQ = 2.8 for 3-I-α-lapachone; RQ = 80.8 for 3-I-β-lapachone; RQ = 4302.5 for doxorubicin) were also upregulated. At least three genes related to the mitogen-activated protein kinase (MAPK) pathway, including *JUN* (RQ = 4.5 for β-lapachone; RQ = 51.8 for 3-I-β-lapachone; RQ = 6603.6 for doxorubicin), *MAPK3* (RQ = 5.3 for β-lapachone; RQ = 25.7 for 3-I-β-lapachone; RQ = 545.6 for doxorubicin), and *MAPK8* (RQ = 3.2 for β-lapachone; RQ = 37.7 for 3-I-β-lapachone; RQ = 682.4 for DOX), were upregulated. Among the genes associated with the Ras oncogene family, *HRAS* (RQ = 3.0 for β-lapachone; RQ = 28.1 for 3-I-β-lapachone; RQ = 392.2 for doxorubicin) and *SOS1* (RQ = 3.6 for β-lapachone; RQ = 49.9 for 3-I-β-lapachone; RQ = 781.0 for doxorubicin) were upregulated. Genes related to cancer immunology, including *NFKB1* (RQ = 3.0 for β-lapachone; RQ = 11.7 for 3-I-β-lapachone; RQ = 536.3 for doxorubicin), *TCF3* (RQ = 3.3 for β-lapachone; RQ = 58.3 for 3-I-β-lapachone; RQ = 146.8 for doxorubicin), and *TGFB1* (RQ = 4.8 for β-lapachone; RQ = 52.2 for 3-I-β-lapachone; RQ = 1930.2 for doxorubicin) were upregulated. In contrast, β-lapachone induced down-regulation of the *PIK3R1* gene (RQ = 0.4 for β-lapachone; RQ = 32.1 for doxorubicin), whereas 3-I-β-lapachone treatment yielded levels similar to those of the control (RQ = 2.4). 3-I-α-Lapachone treatment

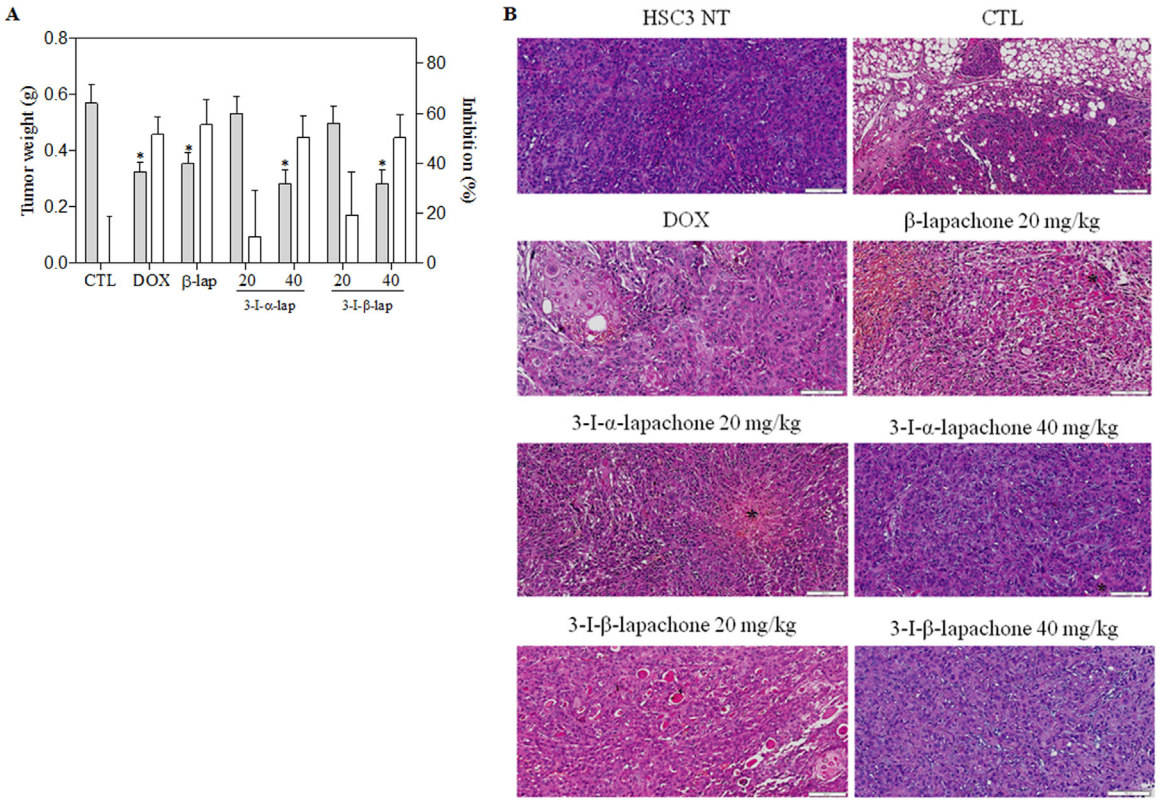

Fig. 6. In vivo antitumor activity of the β-lapachone and its 3-iodine derivatives in C.B-17 SCID mice with HSC3 cell xenografts. a. Quantification of tumor weight and tumor inhibition. The gray bars represent tumor weight (g) and the white bars represent tumor inhibition (%). Data are presented as the means ± S.E.M. of 15–26 animals. * $p < 0.05$ compared with the negative control by ANOVA, followed by the Student–Newma–Keuls test. **b.** Representative histological analysis of the tumors stained with hematoxylin and eosin and analyzed by light microscopy. HSC3 NT is the tumor without treatment. Tumors showed a solid pattern with infiltrative borders and intense cellularity in all groups. Neoplastic cells exhibited large, central, and often vesiculous nuclei with several nucleoli and prominent cytoplasm, which were arranged to form proliferating islands. The asterisks represent tumor necrosis. The negative control (CTL) was treated with the vehicle (5% DMSO) used for diluting the compounds tested. Doxorubicin (DOX, 0.1 mg/kg) was used as positive control. Beginning 72 h after tumor implantation, the animals were treated through the intraperitoneal route for 27 consecutive days.

upregulated the *SPP1* gene (RQ = 13.3 for 3-I-α-lapachone; RQ = 0 for doxorubicin) and downregulated the *PIK3R1* gene (RQ = 0.2 for 3-I-α-lapachone; RQ = 32.1 for doxorubicin). The levels of other genes were similar to those of the control after treatment with 3-I-α-lapachone.

3.7. β-Lapachone and its 3-iodine derivatives reduced HSC3 cell growth in a xenograft model

The CB17 SCID mice were inoculated with HSC3 cells. Seventy-two hours later, treatment was initiated for 27 consecutive days. The animals were treated with β-lapachone at a dose of 20 mg/kg and its 3-iodine derivatives at doses of 20 and 40 mg/kg. Fig. 6**a** shows tumor weights and inhibition percentages after treatment with β-lapachone and its 3-iodine derivatives. Notably, significant reductions in tumor growth were observed for animals treated with doxorubicin (positive control), β-lapachone, and its 3-iodine derivatives, at a dose of 40 mg/kg, when compared with the negative control group (5% DMSO).

Histological analysis demonstrated that tumors showed a solid pattern with infiltrative borders and intense cellularity in all groups. Neoplastic cells exhibited large, central, and often vesiculous nuclei with several nucleoli and prominent cytoplasm, which were arranged to form proliferating islands. In addition, lower frequencies of tumor embolism and inflammation were observed in groups treated with the compounds when compared with the negative control (Fig. 6**b**).

The systemic toxic effects of β-lapachone and its 3-iodine derivatives were evaluated after 27 days of daily treatment. No significant differences were found in body weights and organ wet weights (liver, kidneys, lungs, and heart; Table S3) or in hematological (Table S4) and biochemical (Table S5) parameters after treatment.

Morphological analyses of the liver, kidneys, lungs, and heart in all groups were unremarkable. In the liver, the acinar architecture and centrilobular vein were also preserved in all groups. The chronic inflammation observed in the liver portal space was discrete in most animals. In addition, a lower frequency of inflammatory cells was observed in animals treated with 3-iodine derivatives. Other findings, such as congestion, hydropic degeneration, and steatosis were found in all groups, ranging from mild to moderate (Fig. S7). In the kidneys, tissue architecture was maintained in all experimental groups. In the kidneys of animals, histopathological changes included vascular congestion and glomerular hyalinization, which were observed in all groups treated with the compounds (Fig. S8). In the lungs, the architecture of the parenchyma ranged from partially maintained to modified in all groups. Histopathological changes in all animals ranged from mild to severe. Significant acute inflammation, edema, congestion, hemorrhage, and increased airspace were frequently observed. Importantly, the groups treated with the compounds had a lower frequency of tumor nodules than the negative control group (Fig. S9). Histopathological analysis of animal hearts did not show alterations in any group. Some histopathological features in this study (hydropic degeneration, vascular congestion, and focal areas of inflammation) were acute cellular responses to stimuli unrelated to the treatment, and the injured cells were able to return to a homoeostatic state when the stimulation ended.

4. Discussion

Natural products are main sources of new compounds for the development of drugs with anticancer potential [33]. Thus, in this study, we aimed to evaluate the effects of β-lapachone and its 3-iodine derivatives on cell proliferation, cell death, and cancer-related gene expression in OSCC cells. Importantly, the anticancer activities of the new 3-iodine derivatives were evaluated for the first time in this study.

Assessment of the cytotoxicity of β-lapachone and its derivatives demonstrated that these drugs had promising cytotoxicity in several human cancer cell lines, showing IC_{50} values of less than 4 μg/mL [34,35]. In addition, differences in IC_{50} values between the different cancer cell lines can be justified by tumor heterogeneity and molecular complexity of many types of cancer. Conventional anticancer agents accumulate in normal and cancer cells owing to the lack of specificity. Therefore, the ultimate goal of cancer therapy is to reduce systemic toxicity and improve patients' quality of life [36]. In this regard, β-lapachone and its 3-iodine derivatives showed more potent cytotoxicity for cancer cells than for noncancer cells. Some cancer cells lines were less sensitive to doxorubicin cytotoxicity than non-cancer cells. To confirm the results of cytotoxicity assays, we evaluated viable cell numbers via membrane integrity analysis. β-Lapachone and its 3-iodine derivatives significantly reduced the number of viable HSC3 cells 12 h after treatment. In addition, morphological changes, as assessed by light microscopy and flow cytometry, demonstrated that the compounds reduced the cell volume and increased nuclear fragmentation and chromatin condensation.

The use of three-dimensional (3D) culture models, cell-repellent surface plates, collagen gels, or more complex systems representing the extracellular matrix, such as Matrigel, has been recommended to provide a better assessment of cytotoxicity in the tumor microenvironment by mimicking in vivo models [37]. Thus, 3D model of sphere formatted by HSC3 cells using plates with cell-repellent surfaces and Matrigel to provide a better assessment of cytotoxicity in the tumor microenvironment by mimicking in vivo models. The morphological changes observed 72 h after treatment with β-lapachone and its 3-iodine derivatives indicated that these drugs were cell permeable in the 3D culture that mimics the in vivo cancer tissue. However, the IC_{50} values of the tested compounds and doxorubicin were higher than the IC_{50} values of the two-dimensional model. This higher drug resistance may be due to the presence of the extracellular matrix. In fact, a higher resistance to doxorubicin was also observed in a 3D model using osteosarcoma cells and was associated with the presence of the extracellular matrix, which hinders the release of the drug into the cell [38].

β-Lapachone and its 3-iodine derivatives induced cell cycle arrest at G_2/M phase, followed by increased internucleosomal DNA fragmentation. Similarly, in vitro studies with gastric carcinoma cells [39], lung cancer cells [11], and OSCC cells [21] have demonstrated significant increases in DNA fragmentation after treatment with β-lapachone. Thus, our findings provided support for the mechanism of action of these compounds, by acting on the cell cycle.

In tumors, the amplification and hyperactivation of cyclins and cyclin-dependent kinases (CDKs) or the deregulation of inhibitors of CDKs contribute to cell cycle dysregulation, culminating in cell proliferation [40,41]. In this study, treatment with 3-I-α-lapachone downregulated *CCND2*, but had no effect on *CCND1*, *CCND3*, and *CDK4* transcripts compared with those in the control group. Some chemotherapeutics inhibit the activities of cyclins and CDKs by activating inhibitors of these proteins [42–44]. In this study, treatment with β-lapachone promoted overexpression of the *p21* gene, a CDK1A inhibitor, when compared with the negative control. Consistent with this result, an increase in p21 protein expression was observed in β-lapachone-treated prostate cancer cells [45,46]. In addition, treatment with 3-I-β-lapachone increased the expression of CDKN1A, CDKN1B, and CDKN2A inhibitor transcripts.

Notably, we found that 3-I-β-lapachone also induced apoptosis in OSCC cells. Additionally, overexpression of pro-apoptotic genes, such as the extrinsic pathway receptor (FAS), BAX, and the initiator caspases-8 and -9, was observed compared with the negative control, suggesting that apoptosis may be the main mechanism for 3-I-β-lapachone-induced cell death. Cells treated with β-lapachone and 3-I-α-lapachone showed significant annexin V labeling, further supporting that cell death occurred via apoptosis in these cells. In addition, we observed that pretreatment with a pan-caspase inhibitor was able to significantly reduce apoptosis in HSC3 cells 72 h after treatment with β-lapachone and its 3-iodine derivatives. Importantly, mitochondria play key roles in the physiology and survival of cancer cells, providing energy and metabolites for proliferation and metastasis [47]. Our analysis also showed that the compounds reduced mitochondrial membrane potential, thereby indicating that the apoptosis observed in HSC3 cells was induced by the intrinsic or mitochondrial pathway.

Increased ROS production is one of the main mechanisms of action of many anticancer agents capable of inducing tumor cell death and thus represents an effective strategy for cancer therapy [47]. Within this context, we observed that β-lapachone and its 3-iodine derivatives significantly increased the levels of ROS, particularly hydrogen peroxide, in HSC3 cells 1 h after treatment. In addition, pretreatment with the antioxidant NAC prevented the apoptosis induced by the compounds, indicating the occurrence of ROS-mediated apoptosis.

Some signaling pathways play a key role in the development and progression of cancer. Because activation of Akt increases cell survival by inhibiting pro-apoptotic proteins and activating anti-apoptotic proteins, the phosphatidylinositol-3-kinase/serine-threonine kinase (PI3K/AKT) signaling pathway has great importance as a therapeutic target in cancer [39]. In the current study, cells treated with β-lapachone and 3-I-α-lapachone showed downregulation of *PIK3CA* and *PIK3R1* genes. Furthermore, downregulation of *AKT2*, revealing inhibition of the PI3K/AKT pathway, was observed in cells treated with 3-I-α-lapachone. Thus, these findings provided important insights into the molecular mechanisms through which these compounds exerted their antiproliferative and apoptotic effects.

Based on the promising in vitro results with β-lapachone and its 3-iodine derivatives, we also evaluated the effects and in vivo efficacy of these compounds using a xenograft model. Our results showed that treatment with β-lapachone and its 3-iodine derivatives significantly decreased tumor burden with no toxic effects. This result was consistent with previous findings in mice transplanted with breast adenocarcinoma cells and treated with β-lapachone [8,9].

In summary, our results suggested that β-lapachone and its 3-iodine derivatives displayed promising in vitro and in vivo anticancer potential, contributing to pharmacological studies aimed at the development of new chemotherapeutics drugs. Our findings further revealed the mechanisms through which these compounds exerted their cytotoxic effects, i.e., via promotion of cell cycle arrest at G_2/M phase, internucleosomal DNA fragmentation and promote caspase- and ROS-mediated apoptosis in HSC3 cells. In addition, β-lapachone and its 3-iodine derivatives were able to suppress tumor growth in vivo, indicating that these compounds may be new antitumor drug candidates.

Acknowledgements

The authors are grateful to the flow cytometry, histotechnology and electron microscopy platforms of FIOCRUZ-Bahia for collecting the flow cytometric data, performing the histological techniques and acquiring the photomicrographies. We also thank to Allan Dantas Borges for technical assistance with the graphical abstract.

Funding

This work received financial support and fellowships from Brazilian Agencies, Conselho Nacional de Desenvolvimento Científico e Tecnológico (CNPq) and Fundação de Amparo à Pesquisa do Estado da

Bahia (FAPESB).

Authors' contributions

- Substantial contribution to conception and design: RBD, CAGR, DPB, RDC, MGR, MBPS;
- Performed the synthesis and structural characterization of β-lapachone and its 3-iodine derivatives (3-I-α-lapachone and 3-I-β-lapachone): CAC, TMSS, JMBF;
- Design, acquisition, analysis and interpretation of qPCR data: CAGR, CBSS, LFV;
- Design, acquisition, analysis and interpretation of in vitro studies: RBD, TBSA, RDF, CAGR, DPB, RDC, MGR, MBPS;
- Design, acquisition, analysis and interpretation of in vivo studies: RBD, DPB, EAGR, LPS, ACBCR;
- Contributed reagents/materials/analysis tools: CAGR, DPB, RDC, MBPS, CAC;
- Wrote the paper: RBD, CAGR, DPB;
- Final approval of the version to be published: CAGR, DPB, EAGR, RDC, MGR, MBPS, CAC, JMBF.

Conflict of interest

The authors declare that they have no conflict of interest.

Appendix A. Supplementary material

Supplementary data associated with this article can be found in the online version at doi:10.1016/j.freeradbiomed.2018.07.022.

References

[1] A. Jemal, F. Bray, M.M. Center, J. Ferlay, E. Ward, D. Forman, Global cancer statistics, CA Cancer J. Clin. 61 (2) (2011) 69–90.

[2] P.C. Rodrigues, M.C. Miguel, E. Bagordakis, F.P. Fonseca, S.N. de Aquino, A.R. Santos-Silva, M.A. Lopes, E. Graner, T. Salo, L.P. Kowalski, R.D. Coletta, Clinicopathological prognostic factors of oral tongue squamous cell carcinoma: a retrospective study of 202 cases, Int. J. Oral Maxillofac. Surg. 43 (7) (2014) 795–801.

[3] S. Marur S, A.A. Forastiere, Head and neck squamous cell carcinoma: update on epidemiology, diagnosis, and treatment, Mayo Clin. Proc. 91 (3) (2016) 386–396.

[4] S.N. Sunassee, C.G. Veale, N. Shunmoogam-Gounden, O. Osoniyi, D.T. Hendricks, M.R. Caira, J.A. de la Mare, A.L. Edkins, A.V. Pinto, E.N. da Silva Júnior, M.T. Davies-Coleman, Cytotoxicity of lapachol, β-lapachone and related synthetic 1,4-naphthoquinones against oesophageal cancer cell, Eur. J. Med. Chem. 62 (2013) 98–110.

[5] S. Fiorito, F. Epifano, C. Bruyère, V. Mathieu, R. Kiss, S. Genovese, Growth inhibitory activity for cancer cell lines of lapachol and its natural and semi-synthetic derivatives, Bioorg. Med. Chem. Lett. 24 (2) (2014) 454–457.

[6] A.R. Schuerch, W. Wehrli, Beta-lapachone, an inhibitor of oncornavirus reverse transcriptase and eukaryotic DNA polymerase-alpha. Inhibitory effect, thiol dependence and specificity, Eur. J. Biochem. 84 (1) (1978) 197–205.

[7] M.M. Sitônio, C.H. Carvalho Júnior, A. Campos Ide, J.B. Silva, C. Lima Mdo, A.J. Góes, M.B. Maia, P.J. Rolim Neto, T.G. Silva, Anti-inflammatory and anti-arthritic activities of 3,4-dihydro-2,2-dimethyl-2H-naphthol[1,2-b]pyran-5,6-dione (β-lapachone), Inflamm. Res. 62 (1) (2013) 107–113.

[8] S. Seoane, P. Díaz-Rodríguez, J. Sendon-Lago, R. Gallego, R. Pérez-Fernández, M. Landin, Administration of the optimized β-Lapachone-poloxamer-cyclodextrin ternary system induces apoptosis, DNA damage and reduces tumor growth in a human breast adenocarcinoma xenograft mouse model, Eur. J. Pharm. Biopharm. 84 (3) (2013) 497–504.

[9] Y. Yang, X. Zhou, M. Xu, J. Piao, Y. Zhang, Z. Lin, L. Chen, β-lapachone suppresses tumour progression by inhibiting epithelial-to-mesenchymal transition in NQO1-positive breast cancers, Sci. Rep. 7 (1) (2017) 2681.

[10] H.N. Kung, T.Y. Weng, Y.L. Liu, K.S. Lu, Y.P. Chau, Sulindac compounds facilitate the cytotoxicity of β-lapachone by up-regulation of NAD(P)H quinone oxidoreductase in human lung cancer cells, PLoS One 9 (2) (2014) e88122.

[11] Y.J. Jeon, W. Bang, Y.H. Choi, J.H. Shim, J.I. Chae, Beta-lapachone suppresses non-small cell lung cancer proliferation through the regulation of specificity protein 1, Biol. Pharm. Bull. 38 (9) (2015) 1302–1308.

[12] Y. Wu, X. Wang, S. Chang, W. Lu, M. Liu, X. Pang, β-Lapachone induces NAD(P)H:quinone oxidoreductase-1- and oxidative stress-dependent heat shock protein 90 cleavage and inhibits tumor growth and angiogenesis, J. Pharmacol. Exp. Ther. 357 (3) (2016) 466–475.

[13] C.S. Breton, D. Aubry, V. Ginet, J. Puyal, M. Heulot, C. Widmann, M.A. Duchosal, A. Nahimana, Combinative effects of β-Lapachone and APO866 on pancreatic cancer cell death through reactive oxygen species production and PARP-1 activation, Biochimie 116 (2015) 141–153.

[14] M.S. Beg, X. Huang, M.A. Silvers, D.E. Gerber, J. Bolluyt, V. Sarode, F. Fattah, R.J. Deberardinis, M.E. Merritt, X.J. Xie, R. Leff, D. Laheru, D.A. Boothman, Using a novel NQO1 bioactivatable drug, beta-lapachone (ARQ761), to enhance chemotherapeutic effects by metabolic modulation in pancreatic cancer, J. Surg. Oncol. 116 (1) (2017) 83–88.

[15] H.J. Woo, K.Y. Park, C.H. Rhu, W.H. Lee, B.T. Choi, G.Y. Kim, Y.M. Park, Y.H. Choi, Beta-lapachone, a quinone isolated from Tabebuia avellanedae, induces apoptosis in HepG2 hepatoma cell line through induction of Bax and activation of caspase, J. Med. Food 9 (2) (2006) 161–168.

[16] E.J. Park, K.J. Min, T.J. Lee, Y.H. Yoo, Y.S. Kim, T.K. Kwon, β-Lapachone induces programmed necrosis through the RIP1-PARP-AIF-dependent pathway in human hepatocellular carcinoma SK-Hep1 cells, Cell Death Dis. 5 (2014) e1230.

[17] B.T. Choi, J. Cheong, Y.H. Choi, Beta-lapachone-induced apoptosis is associated with activation of caspase-3 and inactivation of NF-kappaB in human colon cancer HCT-116 cells, Anticancer Drugs 14 (10) (2003) 845–850.

[18] J.Y. Kee, Y.H. Han, J. Park, D.S. Kim, J.G. Mun, K.S. Ahn, H.J. Kim, J.Y. Um, S.H. Hong, β-Lapachone inhibits lung metastasis of colorectal cancer by inducing apoptosis of CT26 cells, Integr. Cancer Ther. 16 (4) (2017) 585–596.

[19] W. Bang, Y.J. Jeon, J.H. Cho, R.H. Lee, S.M. Park, J.C. Shin, N.J. Choi, Y.H. Choi, J.J. Cho, J.M. Seo, S.Y. Lee, J.H. Shim, J.I. Chae, β-lapachone suppresses the proliferation of human malignant melanoma cells by targeting specificity protein 1, Oncol. Rep. 35 (2) (2016) 1109–1116.

[20] J.Y. Kee, Y.H. Han, D.S. Kim, J.G. Mun, S.H. Park, H.S. So, S.J. Park, R. Park, J.Y. Um, S.H. Hong, β-Lapachone suppresses the lung metastasis of melanoma via the MAPK signaling pathway, PLoS One 12 (5) (2017) e0176937.

[21] Y.J. Jeon, W. Bang, J.C. Shin, S.M. Park, J.J. Cho, Y.H. Choi, K.S. Seo, N.J. Choi, J.H. Shim, J.I. Chae, Downregulation of Sp1 is involved in β-lapachone-induced cell cycle arrest and apoptosis in oral squamous cell carcinoma, Int. J. Oncol. 46 (6) (2015) 2606–2612.

[22] R.M.P. Antunes, E.O. Lima, M.S.V. Pereira, C.A. Camara, T.A. Arruda, R.M.R. Catão, T.P. Barbosa, X.P. Nunes, C.S. Dias, T.M.S. Silva, In vitro antimicrobial activity and determination of the minimum inhibitory concentration (MIC) of phytochemicals and synthetic products on bacteria and yeast fungi (Portuguese), Rev. Bras. Farmacogn. 16 (4) (2006) 517–524.

[23] J.M. Barbosa Filho, C.A. Camara, T.M.S. Silva, A.M. Giulietti, M.B.P. Soares, R.R. Santos, Synthesis of 3-iodine-alpha-lapachone and 3-iodine-β-lapachone and uses as biomodulator, antimicrobial and anti-inflammatory (Portuguese), Rev. Prop. Ind. (2006).

[24] P. Boukamp, R.T. Petrussevska, D. Breitkreutz, J. Hornung, A. Markham, N.E. Fusenig, Normal keratinization in a spontaneously immortalized aneuploid human keratinocyte cell line, J. Cell. Biol. 106 (3) (1988) 761–771.

[25] J.P. Jacobs, C.M. Jones, J.P. Baille, Characteristics of a human diploid cell designated MRC-5, Nature 227 (5254) (1970) 168–170.

[26] S.A. Ahmed, R.M. Gogal Jr, J.E. Walsh, A new rapid and simple non-radioactive assay to monitor and determine the proliferation of lymphocytes: an alternative to [3H]thymidine incorporation assay, J. Immunol. Methods 170 (2) (1994) 211–224.

[27] N.C. de Carvalho, S.P. Neves, R.B. Dias, L.F. Valverde, C.B.S. Sales, C.A.G. Rocha, M.B.P. Soares, E.R. dos Santos, R.M.M. Oliveira, R.M. Carlos, P.C.L. Nogueira, D.P. Bezerra, A novel ruthenium complex with xanthoxylin induces S-phase arrest and causes ERK1/2-mediated apoptosis in HepG2 cells through a p53-independent pathway, Cell Death Dis. 9 (2) (2018) 79.

[28] I. Nicoletti, G. Migliorati, M.C. Pagliacci, F. Grignani, C. Riccardi, A rapid and simple method for measuring thymocyte apoptosis by propidium iodide staining and flow cytometry, J. Immunol. Methods 139 (2) (1991) 271–279.

[29] Z. Ni, S. Hou, C.H. Barton, N.D. Vaziri, Lead exposure raises superoxide and hydrogen peroxide in human endothelial and vascular smooth muscle cells, Kidney Int. 66 (6) (2004) 2329–2336.

[30] H. Kojima, N. Nakatsubo, K. Kikuchi, S. Kawahara, Y. Kirino, H. Nagoshi, Y. Hirata, T. Nagano, Detection and imaging of nitric oxide with novel fluorescent indicators: diaminofluoresceins, Anal. Chem. 70 (13) (1998) 2446–2453.

[31] L.S. Glass, A. Bapat, M.R. Kelley, M.M. Georgiadis, E.C. Long, Semi-automated high-throughput fluorescent intercalator displacement-based discovery of cytotoxic DNA binding agents from a large compound library, Bioorg. Med. Chem. Lett. 20 (5) (2010) 1685–1688.

[32] K.J. Livak, T.D. Schmittgen, Analysis of relative gene expression data using real-time quantitative PCR and the 2(-Delta Delta C(T)) Method, Methods 25 (4) (2001) 402–408.

[33] J.H. Kim, Z. Feng, J.D. Bauer, D. Kallifidas, P.Y. Calle, S.F. Brady, Cloning large natural product gene clusters from the environment: piecing environmental DNA gene clusters back together with TAR, Biopolymers 93 (9) (2010) 833–844.

[34] M. Suffness, J.M. Pezzuto, Assays related to cancer drug discovery, in: K. Hostettmann. (Ed.), Methods in Plant Biochemistry: Assays for Bioactivity, Academic Press, London, 1990.

[35] J. Boik, Natural Compounds in Cancer Therapy, Oregon Medical Press, Minnesota, USA, 2001.

[36] A.K. Mitra, V. Agrahari, A. Mandal, K. Cholkar, C. Natarajan, S. Shah, M. Joseph, H.M. Trinh, R. Vaishya, X. Yang, Y. Hao, V. Khurana, D. Pal, Novel delivery approaches for cancer therapeutics, J. Control Release 219 (2015) 248–268.

[37] F. Bonnier, M.E. Keating, T.P. Wróbel, K. Majzner, M. Baranska, A. Garcia-Munoz, A. Blanco, H.J. Byrne, Cell viability assessment using the Alamar blue assay: a comparison of 2D and 3D cell culture models, Toxicol. Vitr. 29 (1) (2015) 124–131.

[38] R. Harisi, J. Dudas, J. Nagy-Olah, F. Timar, M. Szendroi, A. Jeney, Extracellular matrix induces doxorubicin-resistance in human osteosarcoma cells by suppression of p53 function, Cancer Biol. Ther. 6 (8) (2007) 1240–1246.

[39] H.Y. Yu, S.O. Kim, C.Y. Jin, G.Y. Kim, W.J. Kim, Y.H. Yoo, Y.H. Choi, β-lapachone-induced apoptosis of human gastric carcinoma AGS cells is caspase-dependent and regulated by the PI3K/Akt Pathway, Biomol. Ther. 22 (3) (2014) 184–192.
[40] J. Kato, H. Matsushime, S.W. Hiebert, M.E. Ewen, C.J. Sherr, Direct binding of cyclin D to the retinoblastoma gene product (pRb) and pRb phosphorylation by the cyclin D-dependent kinase CDK4, Genes Dev. 7 (3) (1993) 331–342.
[41] R.A. Weinberg, The retinoblastoma protein and cell cycle control, Cell 81 (3) (1995) 323–330.
[42] L. Esposito, P. Indovina, F. Magnotti, D. Conti, A. Giordano, Anticancer therapeutic strategies based on CDK inhibitors, Curr. Pharm. Des. 19 (30) (2013) 5327–5332.
[43] P. Bonelli, F.M. Tuccillo, A. Borrelli, A. Schiattarella, F.M. Buonaguro, CDK/CCN and CDKI alterations for cancer prognosis and therapeutic predictivity, Biomed. Res. Int. (2014) 361020.
[44] C. Sánchez-Martínez, L.M. Gelbert, M.J. Lallena, A. de Dios, Cyclin dependent kinase (CDK) inhibitors as anticancer drugs, Bioorg. Med. Chem. Lett. 25 (17) (2015) 3420–3435.
[45] M.J. Don, Y.H. Chang, K.K. Chen, L.K. Ho, Y.P. Chau, Induction of CDK inhibitors (p21(WAF1) and p27(Kip1)) and Bak in the beta-lapachone-induced apoptosis of human prostate cancer cells, Mol. Pharmacol. 59 (4) (2001) 784–794.
[46] Y.H. Choi, H.S. Kang, M.A. Yoo, Suppression of human prostate cancer cell growth by beta-lapachone via down-regulation of pRB phosphorylation and induction of Cdk inhibitorp21(WAF1/CIP1), J. Biochem. Mol. Biol. 36 (2) (2003) 223–229.
[47] J. Ma, C. Lim, J.R. Sacher, B. Van Houten, W. Qian, P. Wipf, Mitochondrial targeted β-lapachone induces mitochondrial dysfunction and catastrophic vacuolization in cancer cells, Bioorg. Med. Chem. Lett. 25 (21) (2015) 4828–4833.